

THEORETICAL INVESTIGATION OF AN AMMONIA–WATER POWER AND REFRIGERATION THERMODYNAMIC CYCLE

V. POPA¹ C. POPA¹

Abstract: *A combined thermal power and cooling cycle proposed by Goswami is under theoretically investigation. The proposed cycle combines the Rankine and absorption refrigeration cycles, using a binary ammonia–water mixture as the working fluid. This cycle can be used as a bottoming cycle using waste heat from a conventional power cycle or an independent cycle using low temperature sources such as geothermal and solar energy. For a solar heat source, optimization of the second law efficiency is most appropriate, since the spent heat source fluid is recycled through the solar collectors. The optimization results verified that the cycle could be optimized using the generalized reduced gradient method.*

Key words: *thermodynamics, water-ammonia, power, refrigeration.*

1. Introduction

Multi-component working fluids in power cycles exhibit variable boiling temperatures during the boiling process which make them suitable for a sensible heat source [6]. The temperature difference between the heat source and the working fluid remains small to allow for a good thermal match between the source and working fluid, such that less irreversibility results during the heat addition process. A novel ammonia–water binary mixture thermodynamic cycle capable of producing both power and refrigeration has been proposed by Goswami (1998). An ammonia–water mixture is used as it exhibits desirable thermodynamic properties in terms of a large heat capacity. Ammonia is relatively inexpensive, can accommodate system design modifications

well and separates easily from internal lubricating oils. Ammonia is also environmentally benign in comparison to other binary mixtures used in industry. A schematic of the cycle is shown in Fig. 1. The relatively strong basic solution of ammonia–water leaves the absorber as saturated liquid at the cycle low pressure. It is pumped to the system high pressure and is preheated before entering the boiler by recovering heat from the weak solution returning to the absorber. As the boiler operates between the bubble and dew point temperatures of the mixture at the system high pressure, partial boiling produces a high concentration saturated vapor and relatively low concentration saturated liquid. The liquid weak solution gives up heat in the recovery unit and throttles into the absorber. The rectifier condenses out water to further purify the vapor, by

¹ Dept. of Thermotechnics and Thermal Machines, *Dunarea de Jos* University of Galati.

heat added to the cycle from the heat source in both the boiler and superheater. These are calculated based on simple mass and energy balances over the cycle components.

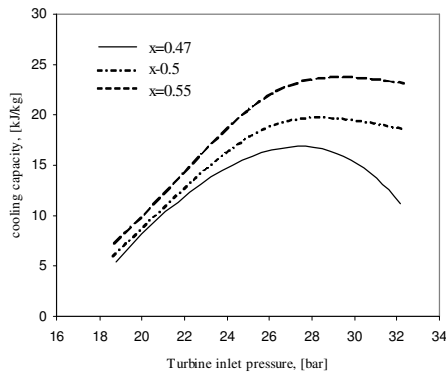


Fig.2. *Effect of turbine inlet pressure on the cooling capacity, [kJ/kg]*

Fig. 2 shows that for higher ammonia mass fractions in the basic solution, more vaporization occurs for the given boiler temperature and pressure. A higher vapor fraction allows for greater flow through the turbine, and more work production for a higher thermal efficiency.

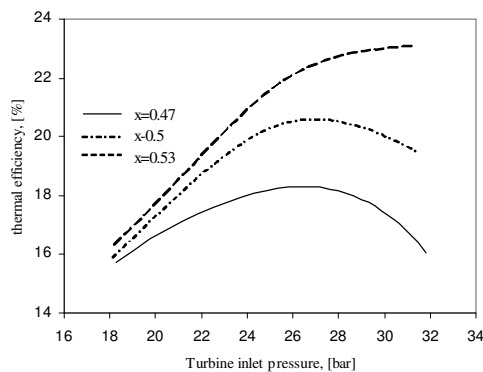


Fig. 3. *Effect of turbine inlet pressure on the thermalefficiency of the cycle*

Fig. 3 concludes that more vapor is available for refrigeration output also, per kg of basic solution that is boiled.

For increasing turbine inlet or system high pressure, the figures show that the work and cooling outputs peak. Determining the location of these peaks is necessary a priori to optimize a working system's performance.

Initially, increasing the system high pressure while holding other parameters constant increases the pressure ratio across the turbine, such that there is more expansion work and lower turbine exit temperatures. However, the effect of the higher pressure limiting vapor production begins to dominate as the boiler exit fluid is shifted towards saturated liquid. The peak shifts for higher basic solution mass fractions as a two-phase equilibrium can be sustained at higher pressures for higher mass fractions.

Figures 2 and 3 were evaluated for a boiler at 400 K, superheater at 410 K, absorber at 280 K and rectifier at 360 K. The low pressure in the system at the absorber was set at 2 bar. For practical operation, the cycle has several parameters that are varied together, presenting a multi-dimensional surface on which an optimum can be found. A mathematical approach at locating this optimum is necessary, as the resulting surface cannot be visualized.

2.2. Optimization

For a solar heat source, optimization of the cycle for maximum second law cycle efficiency is most appropriate as the heat source fluid is recycled back to the solar collectors at a temperature that is higher than the ambient. The unused exergy is not wasted. Exergy, or availability, is defined as the maximum reversible work a substance can do during the process of reaching equilibrium with its environment.

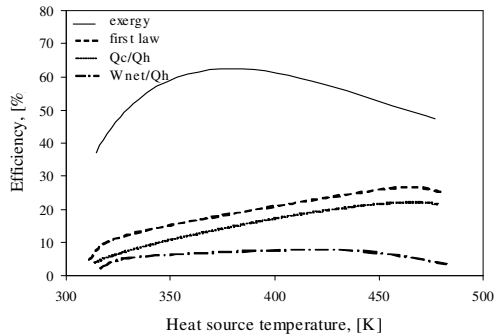


Fig. 4. Efficiencies of the optimized cycle at various heat source temperatures, optimized for second law efficiency

The second law efficiency is defined as the exergy output divided by the exergy input to the cycle [1]. The exergy input is taken as the available energy change of the heat source. The exergy output is the exergy of the net work and the exergy of the refrigeration. The second law or exergy efficiency is given by Eq. (2).

$$\eta_2 = \frac{W_{net} + E_c}{\Delta E_{hs}} \quad (2)$$

The exergy of refrigeration, E_c , is the refrigeration capacity divided by the coefficient of performance of a Carnot refrigeration cycle operating between the ambient and cycle low temperatures, as given by Eq. (3).

$$E_c = Q_c \frac{(T_0 - T_c)}{T_c} \quad (3)$$

2.2.1. Optimization methodology

A generalized reduced gradient (GRG) scheme is used for the optimization [5]. The GRG method searches a feasible region bounded by equality and inequality constraints. Moving finitely towards a better value with a newly determined search direction at every step, the optimum is ultimately reached within a limit of convergence.

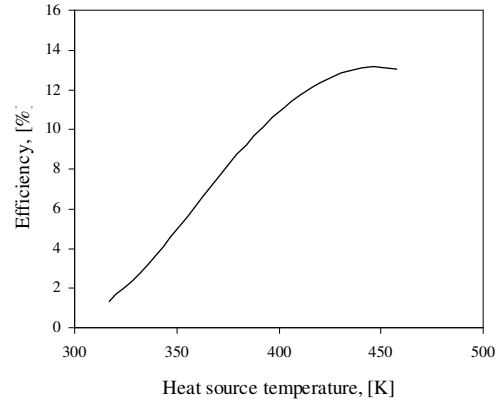


Fig. 5. Pressure ratio of the optimized cycle various source temperatures, optimized for second law efficiency

The optimization scheme searches over eight free variables for the optimal second law efficiency as defined by Eq. (2). The parameters are the absorber or ambient temperature, boiler, superheater and rectifier temperature, the boiler pressure (high pressure), absorber pressure (low pressure), and heat source inlet and exit temperatures. From these eight free variables all other state points in the cycle can be determined with minimal and reasonable assumptions.

2.2.2. Optimization results

The desired heat source temperature will vary according to the intended use of the cycle. The effects of heat source temperature on the optimized cycle performance are shown in Figs. 4–7, optimized for second law efficiency. The refrigeration as a fraction of the heat addition, $Q_c=Q_h$, changes little as the heat source temperature increases as shown in Fig. 4. As the heat source temperature approaches the ambient temperature, refrigeration approaches zero.

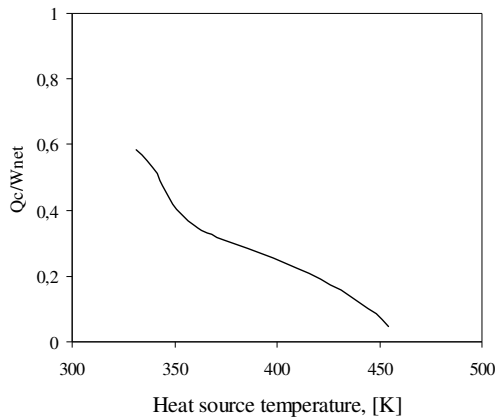


Fig. 6. *Ratio of refrigeration to work of the optimized cycle at various heat source temperatures, optimized for second law efficiency*

The highest refrigeration fraction is near a source temperature of 390 K. The refrigeration fraction decreases to zero near 480 K, as the higher temperature vapor can no longer be expanded to sub-ambient temperatures. The net power as a fraction of heat addition, $W_{net}=Q_h$, increases as the heat source temperature increases. As the turbine work output is related mainly to the pressure ratio across the turbine, the net power curve can be explained in relation to pressure ratio in Fig. 5, which shows a continuous increase with heat source temperature. The first law efficiency curve, which is a sum of the refrigeration and power curves, shows similar behavior to the power curve up to the maximum value of 23.6% at 400 K. After the maximum point, the efficiency starts decreasing slowly in a similar manner to the refrigeration curve.

The second law or exergy efficiency shows a maximum value of 65.2% at 380 K. The sharp increase in Fig. 4 of the second law efficiency between 320 and 380 K is due to the increase of both power and refrigeration outputs. The second law efficiency reaches a maximum where the refrigeration output begins to decrease above 400 K.

Fig. 6 shows the refrigeration to net power ratio versus the heat source temperature. In the temperature range between 320 and 360 K this ratio changes rapidly, while above 360 K the ratio decreases slowly, reaching 0.12 at 460 K. Thus, increasing the heat source temperature favors the production of power rather than refrigeration.

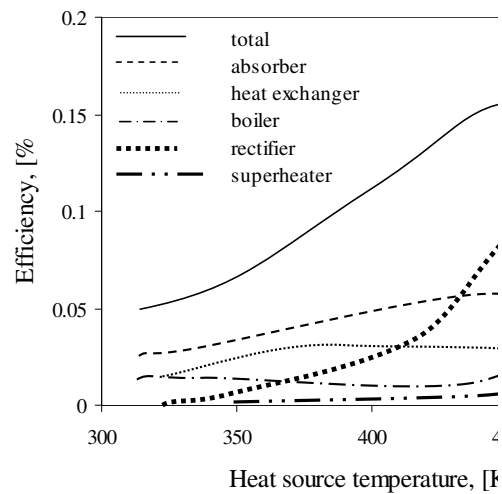


Fig. 7. *Exergy destruction of the optimized cycle at various heat source temperatures, optimized for second law efficiency*

Fig. 7 shows the normalized exergy destruction in the cycle as a function of the heat source temperature. The total exergy destruction in the cycle increases with an increase in the heat source temperature. It can be seen in Fig. 7 that the exergy destruction in both the absorber and heat exchanger changes little as the source temperature increases. The superheater has almost no exergy destruction because of its small heat load. The boiler exergy destruction is much lower than that of the absorber. Exergy destruction in the rectifier increases throughout, as the heating load also increases in the rectifier. From the exergy analysis, if the heat

source is between 320 and 460 K, then the best operating heat source temperature is around 380 K, since it gives the maximum exergy efficiency. It has been shown that the cycle can be optimized for a range of heat source temperatures. Similarly, the cycle can be optimized for each heat sink or ambient temperature, and other parameters. Therefore, the cycle can be customized to the intended application for optimal performance.

2.3. Irreversibility analysis

In realistic systems, there are irreversibilities associated with every component as with this ammonia–water cycle. These irreversibilities will have negative effects on the performance of the cycle. The effects of each loss were studied individually and jointly on the cycle performance. Typical working conditions used in this analysis were 400 K and 30 bar at the boiler exit, 360 K rectification, 410 K at the turbine inlet, 280 K and 2 bar in the absorber, and a basic solution mass fraction of 0.53.

A typical turbine efficiency of 90% was assumed as suggested in the literature [2]. The thermal efficiency drops from 23.3% to 19.7%, a decrease of 15.4%. Due to the irreversibility in the turbine, although the pressure ratio is the same, the exhaust temperature of the turbine is higher. Less energy is converted into mechanical work in the turbine, and the turbine work output drops from 76.1 to 68.5 kW, a decrease of 10.0%. At the same time, a higher turbine exhaust temperature provides less cooling capacity. The cooling capacity drops 29.2% from 26.0 to 18.4 kW. An 80% pump efficiency was assumed as suggested in the literature [2]. The pump work requirement increases from 3.4 to 4.2 kW. This small increase causes the thermal efficiency to drop slightly. A pressure loss of 5% of the inlet pressure was assumed

across the boiler. The results show this pressure loss has almost no negative effect on the cycle performance. Only slightly more pump work is required to boost the boiler inlet pressure to compensate for the pressure loss in the boiler. A pressure loss of 5% was assumed for the superheater. The results show only a minor negative effect on the cycle performance. Thermal efficiency decreases by 3% of that in the ideal cycle, from 23.3% to 22.6%. Due to the pressure loss in the superheater, the turbine inlet pressure drops. Therefore, less expansion is possible producing 1.2% less work and higher exhaust temperatures. The cooling capacity decreases by 6.5%. A pressure loss of 5% was assumed for both streams in the recovery heat exchanger. The effects on the cycle performance are minimal, with a negligible decrease in thermal efficiency owing to an increase in the pump work requirement. A pressure loss of 5% was assumed in the refrigeration heat exchanger, for comparison to other component pressure losses. The thermal efficiency drops by 2.6% from 23.3% to 22.7%, as the higher turbine exhaust pressure limits the expansion possible. The work output decreases by 1.6%. The reduced turbine pressure ratio also raises the exhaust temperature, reducing the cooling capacity by 4.6%. In a typical cooler, however, the heat exchanger experiences a 3% pressure loss, which is the value used in the combined irreversibility study.

Finally, the overall effect of the irreversibility associated with the cycle was analyzed for combined losses. The thermal efficiency decreases by 20.6%, from 23.3% under ideal conditions to 18.5%. The turbine work output drops by 11.8%, from 76.1 to 67.1 kW. The cooling capacity decreases by 37.7%, from 26.0 to 16.2 kW. It can be seen that the greatest loss is attributed to the expansion in the turbine not being isentropic.

3. Conclusions

Parametric analysis of the cycle showed the potential for the cycle to be optimized. Optimization of the operating parameters in the cycle is possible for each heat source and heat sink temperature, using a GRG method. The cycle may be optimized for the first law efficiency, second law efficiency, power output or cooling output, depending on the intended application and the heat source. For a solar heat source, optimization for the second law efficiency is most appropriate, since the spent heat source fluid is recycled back to the solar collectors. It was found from simulation that optimization of the cycle for second law efficiency produces no refrigeration at high heat source temperatures, while for low heat source temperatures it does. Inclusion of realistic losses in the analysis of the cycle reduces the cycle thermal efficiency by 20.6%, with 11.8% less work output and 37.7% less cooling capacity. The most significant source of irreversibility in the cycle is a non-isentropic expansion process in the turbine. An experimental system was constructed and successfully operated to demonstrate the feasibility of the combined power and cooling thermodynamic cycle.

The results from test data compared well to simulations. Vapor generation and absorption condensation processes were shown to work experimentally. The potential for combined work and refrigeration output was evidenced. Addition of a turbine/ generator set and a chiller/heat exchanger are needed to confirm this conclusion. An analysis of

losses has shown where improvements can be made, for further testing over a broader range of operating parameters.

References

1. Cengel, Y.A., Boles, M.A.: *Thermodynamic*. In: *Engineering Approach*, third ed. McGraw-Hill Inc., New York, 1998.
2. Drbal, L.F., Boston, P.G., et al.: *Power Plant Engineering*. Chapman & Hall, New York, 1996.
3. Goswami, D.Y., 1998. *Solar thermal technology: present status and ideas for the future*. In: *Energy Sources* 20, 137–145.
4. Goswami, D.Y., Xu, F.: *Analysis of a new thermodynamic cycle for combined power and cooling using low and medium temperature solar collector*. In: *ASME (1999) Journal of Solar Energy Engineering* 121, 91–97
5. Goswami, D.Y., Hasan, A.A., Lu, S., Tamm, G.: *Ammonia-based combined power/cooling cycle*. In: *UFME/SEECL. Report 2001-05*. University of Florida, Gainesville, FL. 2001.
6. Kalina, A.I. *Combined cycle system with novel bottoming cycle*. In: *Journal of Engineering for Gas Turbines and Power* 106, 737–742, 1984.
7. Norton, E.: *Ammonia Liquid Recirculation*. In: *ASHRAE Journal* 43 (10), 50–51, 2001.
8. Xu, F., Goswami, D.Y.: *Thermodynamic Properties of Ammonia Water Mixtures for Use in Power Cycles*. In: *Energy (Oxford)* 24, 525–536, 1999.

